Journal of Control, Automation and Electrical Systems (2018) 29:153–162
https://doi.org/10.1007/s40313-017-0364-5

Automated System for Femtosecond Laser Writing of Photonic Structures

Yujuan Wang[1] · Lucas Hermann Negri[2] · Ismael Chiamenti[1] · Ilda Abe[1] · Hypolito José Kalinowski[3]

Received: 4 July 2017 / Revised: 1 November 2017 / Accepted: 22 December 2017 / Published online: 8 January 2018

Abstract
An automated system is reported in this work with the goal of fabricating photonic structures by the direct-write technique with femtosecond laser pulses. This technique uses a fine focused laser beam into transparent substrates and the translation of the substrate parallel or perpendicular to the propagation direction of the incident laser beam. Control procedures related to laser pulses and the sample translation were implemented and integrated, giving rise to a fully automated femtosecond writing system. Functional straight-line and curved waveguides have been successfully achieved with the automated writing system, where single-mode propagation is observed from their near-field profiles when 635-nm light is injected and guided. In addition, the possibility of writing 2D and 3D photonic structures is confirmed by tracing a logarithmic spiral structure (2D) and a fan-out structure (3D). These results show that the developed system is fully operational in practice for the purpose of fabricating a variety of photonic structures with potential applications in the modern communication networks and integrated photonic circuits.

Keywords Automation · Control · Automated system · Femtosecond laser · Photonic structures · Femtosecond writing technique

1 Introduction

Since the first demonstration of surface ablation using a femtosecond laser in 1994, femtosecond laser micromachining has gone through a period of rapid development and application. This technique can be used either to ablate materials or to change a material's optical properties for the fabrication of photonic structures and devices (Gattass and Mazur 2008).

Traditionally, dating back to the 1970s, UV lasers were employed to photoinduce refractive index changes in transparent materials such as glasses and optical fibers (Davis et al. 1996). In contrast, at that time IR lasers gained little attention because of their low photon energy at this wavelength range, which avoid photoinduced changes in the refractive index. However, with the development of femtosecond pulsed lasers, the process became possible as the intensity of the laser light could be high enough for the nonlinear absorption to occur owing to the ultrashort duration of laser pulses together with the use of focusing devices (e.g., microscope objective). In this case, a nonlinear process, called optical breakdown, can take place whereby the photon energy is transferred to the material via multiphoton absorption and then deposited to the material's lattice via photoionization and plasma relaxation. As a result of the nonlinear process, a permanent refractive index change can be induced inside the irradiated material. Attributing to the nonlinear nature, the photoinduced structural change is microminiaturized and confined to the inside of the focal volume without causing alterations (ablation or damage) at the surface of the irradiated material. Positive refractive index change can be obtained under appropriate irradiation conditions, making it possible to directly write light-guiding structures with IR femtosecond lasers. The first functional waveguide written in glass with a femtosecond IR laser is reported in the work

✉ Yujuan Wang
yujuan.jade@gmail.com

Hypolito José Kalinowski
hjkalinowski@id.uff.br

[1] Federal University of Technology – Paraná (UTFPR), Curitiba 80230-901, Brazil

[2] Federal Institute of Education, Science and Technology of Mato Grosso do Sul (IFMS), Aquidauana 79200-000, Brazil

[3] Departamento de Engenharia de Telecomunicações, Universidade Federal Fluminense (UFF), Niterói 24210-240, Brazil

of Miura in 1997 (Miura et al. 1997). From that point on, femtosecond laser writing of photonic structures and devices emerged as an active area of research.

The direct-write technique with femtosecond lasers provides a straightforward and promising way for the fabrication of light-guiding structures, which is much easier and more time economical when compared to traditional fabrication methods such as physical vapor deposition and ionic exchange (Miura et al. 1997). This is of particular importance in the prototyping stages of new devices.

Another advantage is that the spatial confinement together with a precise computer-controlled translation of the sample enables the straight fabrication of 3D photonic structures and patterns with complex and arbitrary geometries, which are not possible with the commercial optical fiber and lithography technologies (Nolte et al. 2003). In addition, due to the nonlinear absorption, photonic structures can be produced in a variety of transparent materials, including glasses, crystals and polymers.

Generally, the photoinduced refractive index contrast is in the order of 10^{-4}–10^{-3}, which is similar to the case of commercial optical fibers, whereas high permanent refractive index increase in the order of 10^{-2} has been achieved in glass waveguides (Ams et al. 2005; Eaton et al. 2011).

So far, a large number of photonic structures and devices have been successfully fabricated and reported in the literature, including waveguides (Ams et al. 2005; Eaton et al. 2011), splitters and dividers (Nolte et al. 2003; Liu et al. 2005; Sakakura et al. 2010), directional couplers (Chen et al. 2008; Pospiech et al. 2009), multiplexers/demultiplexers (Mauclair et al. 2009), interferometers (Minoshima et al. 2002), Bragg grating filters and sensors (Zhou et al. 2010; Lacraz et al. 2015), Bragg grating waveguides (Marshall et al. 2006), and amplifiers (Sikorski et al. 2000; Valle et al. 2005). Such optical devices are important components in the area of modern optical communication network.

The large majority of functional photonic structures described in the literature were fabricated with a sample translation speed lower than 1 mm s^{-1} due to the need of low laser energy dose of some μJ s. Thus, it can take several hours to accomplish a group of parameter-searching tests. Under this circumstance, it is reasonable to automate the fabrication process for the benefit of saving production time and dispensing the continuous human supervision and operation in the course of experiments.

Optical waveguides in the form of straight lines can be easily written by translating the processed sample in a unique direction. However, 2D or 3D photonic structures usually contain sections of bended waveguides, which could be a delicate problem of engineering as the radius of curvature should be large because of the present bending loss that, in turn, requires a large amount of high-precision motion control commands, in order to trace the expected smooth trajectory with constant energy deposition along the whole path. In such a situation, an automated motion control system is necessary to fulfill the task, since it is inviable to write such a functional curved waveguide in a manual way. It is also worth mentioning that a timely control of laser pulses (blocking or passing) ought to be added into the writing process of some 2D and 3D photonic structures of complex geometries, where fragments are written sequentially and the laser beam should be blocked in fragment intervals to avoid bringing out structural modifications in undesired regions of the processing sample.

This work reports the development of an automated femtosecond writing system for fabricating photonic structures. The automated system contains not only the motion control of samples, but also the on–off control and the power adjustment of laser pulses. To our best knowledge, works covering both the automated movement of the sample and the laser beam power conditions have been rarely presented in the literature, even though there are several laboratory homemade or commercially available laser writing systems around the world. Functional straight-line and S-bend waveguides are fabricated with computer-controlled writing programs. Moreover, the fabrication of 2D and 3D photonic structures is also shown to be available.

2 Experimental Setup

Figure 1 shows a schematic design of the laboratory experimental setup for the femtosecond writing of photonic structures. The laser used in this work is a regenerative amplified 800-nm Ti:Sapphire laser that emits 100 fs, 1 kHZ pulses and delivers a maximum power of 3.24 W. A Thorlabs SH05 optical beam shutter was placed in front of the femtosecond laser, providing millisecond shutter operation (blocking or passing the laser beam). A series of filters and mirrors were inserted along the laser beam path (indicated by red lines) between the laser and the microscope objective,

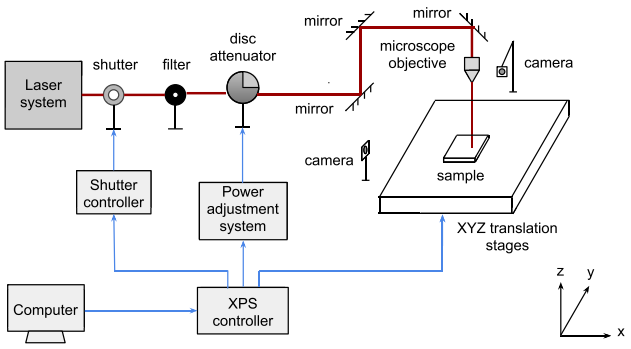

Fig. 1 Schematic design of the experimental setup of femtosecond writing system

which play the role of controlling the average laser power and directing the laser beam until the microscope objective. Laser power was varied and measured through a rotatory disk attenuator and a power meter. Two digital cameras were installed frontally (in *x*-direction) and diagonally (at 45° in the *yz*-plane) for the purpose of monitoring the sample's optical alignment process before the femtosecond writing. This alignment was achieved manually by translating sequentially the sample in *z*, *x* and *y* directions and rotating finely the sample support, making sure the upper and lateral faces of the sample lie in the *xy*-plane, *yz*-plane and *xz*-plane, respectively. The femtosecond laser pulses were tightly focused into processed substrates using a 20× microscope objective with a numerical aperture of 0.4.

Substrates were mounted on a *XYZ* translation group (Newport VP-25XA in *x*-direction, XML-160 in *y*-direction and GTS-30 in *z*-direction), each with a resolution of 100, 10 and 50 nm, respectively. With the help of a XPS motion controller, glass samples were translated in directions parallel and perpendicular to the incident laser beam.

With respect to the automation and control part, the automated femtosecond writing system consists of shutter control, motion control and laser power adjustment control, whose control paths are indicated by blue lines. The power adjustment unit and the motion control unit receive computer-controlled commands independently, and they can communicate with each other via network sockets. The shutter control has two options of configuration (XPS mode and PAU mode), which permit it to be embedded into either the motion control unit or the power adjustment unit (PAU).

For the visual inspection, laser-written structures were imaged with the aid of an optical transmission microscope and a confocal laser scanning microscope (CLSM). The characterization of light-guiding properties of written waveguides was carried out by injecting 635-nm light into the waveguide. The light was emitted from a semiconductor laser (Opnext, HL6320G) and coupled to an optical fiber (Thorlabs, CFS2-532-FC) terminated with a GRIN lens. Two microscope objectives of 10× magnification were used to focus light from fiber into waveguide and capture guided light by waveguide to an optical beam profiler (Thorlabs, BP104-UV). Thus, the waveguide's cross-sectional intensity profiles can be measured for the analysis of the waveguide's light-guiding characteristics.

3 Automation of the Femtosecond Writing System

3.1 Motion Control

The Newport XPS-Q8 is an integrated motion controller. It supports the TCP/IP communication protocol and uses TCP/IP blocking sockets. In this work, motion process programs were written in a way of host-managed processes, that is to say, use the Ethernet TCP/IP interface from a PC to control the XPS. In this case, it is more efficient to control the writing process from a dedicated program that runs on a PC and is more suitable for applications that require data management or digital communication with other devices rather than the XPS. Furthermore, based on the Ethernet TCP/IP communication protocol, the development of motion process programs is independent of the PC's operating system and programming language. The programming language chosen in this work is Python, and the original Python application programming interface (API) is available from the XPS's Python driver.

In this work, three Newport DC motor linear translation stages were connected and driven by the XPS controller. These positioners can be assigned to different motion groups, such as SingleAxis group, XY group and XYZ group. That way, depending on the group configuration, these three positioners can be operated independently to conduct simple point-to-point movements as well as be performed in the XY or XYZ mode to accomplish more complex motion sequences. Once defined, the XPS automatically deals with all safety restrictions and executes trajectories of the motion group.

The XPS controller provides several modes of positioning from simple point-to-point motion to the most complex trajectories. On execution of a motion command, the exact trajectory for the motion is calculated by a sophisticated motion profile that is adopted aiming to eliminate mechanical resonance caused by an abrupt change in acceleration, which occurs in the case of traditional trapezoidal motion profile (trapezoidal velocity profile). Among the various available motion modes, only modes of point-to-point, line–arc and spline trajectories were adopted for the femtosecond writing of photonic structures. The line–arc trajectory defines a 2D trajectory as a combination of linear and circular segments, which is only available for positioners in XY groups. The spline trajectory executes a Catmull–Rom spline (third-degree polynomial curve) on an XYZ group, which permits tracing a smooth 3D curve that passes by all predefined trajectory points. Both of these trajectories are able to maintain constant speed (the scalar part of the trajectory velocity) during the entire path, excepting the acceleration and deceleration periods. However, the discontinuity of line–arc trajectory is categorized as R0, while the Spline has a C^1 continuity. In both cases, the trajectory is user defined in a text file that should be sent to the controller via FTP. Once defined, the user executes a function to start the trajectory execution and the XPS automatically calculates and executes the motion path.

During the execution of a motion process program, motion parameters (position, velocity and acceleration) can be obtained by "getter" functions, which allow precise mon-

itoring of motion all along the traced path. Both set point and current values of these motion parameters are accessible, wherein the former refers to the theoretic values from the motion profiler and the latter refers to the actual values. Upon this functionality, data gathering (synchronous and asynchronous) at up to 10 kHz rate, up to 1,000,000 data entries is also furnished by the XPS controller. Hence, motion parameters during the motion process can be gathered and saved in a gathering file to the flash disk of the XPS controller, in the interest of a later detailed trace analysis. When combined with the event trigger functionality of XPS, different types of motion-related data gathering can be configured with a great flexibility. This kind of used-defined "actions at event" can be monitored by the controller at up to 10 kHz rate. Moreover, multiple digital and analog I/O's from the rear panel of XPS enable users to perform additional data acquisition, synchronization and control features with other devices, for example, triggering the shutter controller in this work.

Using the original Python API provided by the XPS controller, a simple waveguide writing program is shown in Fig. 2, whose flowchart is shown in Fig. 3 ignoring the flow control of exception management. This simple motion process program is designed to write an array of five waveguides with different writing velocities, with the aim of finding the suitable velocity for the waveguide writing. Lines 4–6 specify the experimental parameters: Waveguide writing velocities vary from 5 to 40 μm s^{-1}; high velocity of 1 mm s^{-1} is used to change the positioner to the next waveguide writing position; the space between two adjacent waveguides is 0.5 mm; all the waveguides have the same length of 10 mm. After connecting the PC to the XPS controller, the first thing is to ensure that the shutter is closed, as shown in line 22, preventing the laser beam from arriving at the processed substrate and causing undesirable damages inside the substrate. Lines 26–55 use a repetition loop to write five waveguides with their respective writing velocity, using a few of provided functions of the Python driver. With the embedded function GPIODigitalSet(), a digital TTL output from a general purpose I/O connector is sent to the shutter controller to trigger (open or close) the shutter, as the shutter operates in the XPS mode in this case. Motion profile parameters (velocity, acceleration, minimum and maximum jerk) for a specific positioner can be configured through the function PositionerSGammaParametersSet(). Meanwhile, point-to-point relative move can be done with the function GroupMoveRelative(). In this original API, error handling is performed by verifying the return code of every command issued. It should be observed that error handling is necessary in all motion process programs, since the shutter should be closed immediately in case the controller's security mechanism detects any errors during the motion process. Finally, the connection to the XPS controller should be disconnected after finishing the writing of waveguides.

```
1  import XPS_Q8_drivers, sys, time
2
3  ADDRESS = '192.168.0.254', 5001
4  vels = [0.005, 0.01, 0.02, 0.03, 0.04]
5  vel_high = 1
6  space, length = 0.5, 10
7
8  def close_and_exit(xps, sock, err_code=None):
9      if err_code: print('Error {}'.format(err_code))
10     xps.GPIODigitalSet(sock, 'GPIO1.DO', 1, 0)
11     xps.TCP_CloseSocket(sock)
12     sys.exit()
13
14 if __name__ == "__main__":
15     xps = XPS_Q8_drivers.XPS()
16     sock = xps.TCP_ConnectToServer(IP=ADDRESS[0],
           port=ADDRESS[1], timeOut=30)
17
18     if sock == -1:
19         print("Could not connect")
20         sys.exit()
21
22     err_code, ret = xps.GPIODigitalSet(sock, 'GPIO1
           .DO', 1, 0)
23     if err_code != 0:
24         close_and_exit(xps, sock, err_code)
25
26     for vel in vels:
27         err_code, ret = xps.
               PositionerSGammaParametersSet(sock, '
               Group3.Pos', vel, 2500.0, 0.02, 0.02)
28         if err_code != 0:
29             close_and_exit(xps, err_code)
30
31         err_code, ret = xps.GPIODigitalSet(sock, '
               GPIO1.DO', 1, 1)
32         if err_code != 0:
33             close_and_exit(xps, err_code)
34
35         err_code, ret = xps.GroupMoveRelative(sock,
               'Group3', [length])
36         if err_code != 0:
37             close_and_exit(xps, err_code)
38
39         err_code, ret = xps.GPIODigitalSet(sock, '
               GPIO1.DO', 1, 0)
40         if err_code != 0:
41             close_and_exit(xps, err_code)
42
43         err_code, ret = xps.
               PositionerSGammaParametersSet(sock, '
               Group3.Pos', vel_high, 2500.0, 0.02,
               0.02)
44         if err_code != 0:
45             close_and_exit(xps, err_code)
46
47         err_code, ret = xps.GroupMoveRelative(sock,
               'Group3', [-length])
48         if err_code != 0:
49             close_and_exit(xps, err_code)
50
51         err_code, ret = xps.GroupMoveRelative(sock,
               'Group4', [space])
52         if err_code != 0:
53             close_and_exit(xps, err_code)
54
55         time.sleep(1)
56
57     close_and_exit(xps, sock)
```

Fig. 2 Python code of a simple waveguide writing program

3.2 New Object-Oriented API

A new object-oriented API was developed, taking advantages of modern functionalities of the Python programming language. The new API was introduced to reduce the repetition of code and function parameters as well as to facilitate exception handling. It is implemented as a Python module, which internally makes use of the old API provided by the XPS controller. The writing program example originally seen in Fig. 2 is rewritten by using the new API, which is shown in Fig. 4 for the purpose of comparison.

One of the new API's proposals lies in the use of exceptions to perform error handling without having to repeatedly

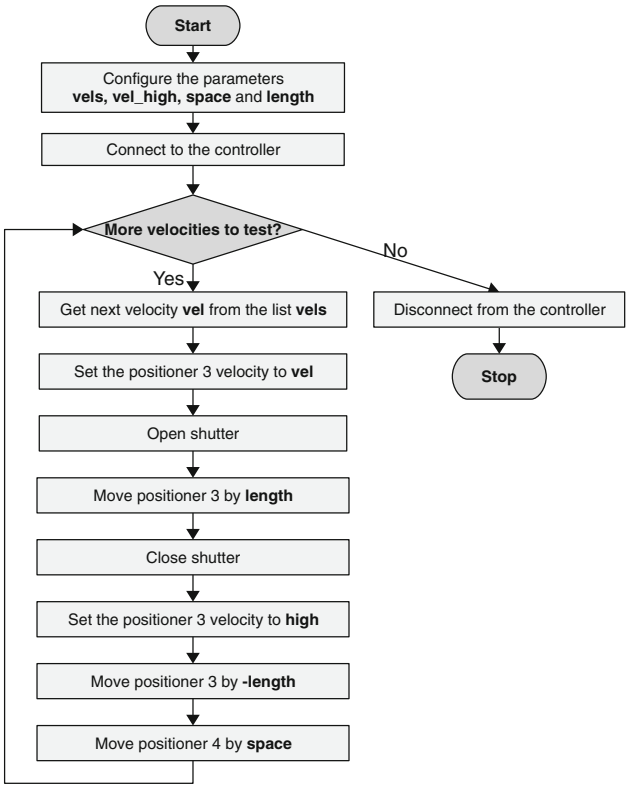

Fig. 3 Flowchart of the writing program in Fig. 2

```
1  from xps import XPS
2  import time
3
4  ADDRESS = '192.168.0.254', 5001
5  vels = [0.005, 0.01, 0.02, 0.03, 0.04]
6  vel_high = 1
7  space, length = 0.5, 10
8
9  if __name__ == '__main__':
10     xps = XPS(ADDRESS)
11
12     with xps.connected():
13         shutter = xps.shutter()
14         shutter.close()
15
16         group3 = xps.group('Group3')
17         group4 = xps.group('Group4')
18         pos3 = group3.positioner()
19         pos4 = group4.positioner()
20
21         for vel in vels:
22             pos3.set_sgamma(vel, 2500.0, 0.02,
                   0.02)
23
24             with shutter.opened():
25                 group3.move_relative(length)
26
27             pos3.set_sgamma(vel_high, 2500.0, 0.02,
                   0.02)
28             group3.move_relative(-length)
29             group4.move_relative(space)
30             time.sleep(1)
```

Fig. 4 Rewrite of the Python source code of the waveguide writing program by using the proposed object-oriented API

check the returned error code for each submitted command. Meanwhile, the new API also proposes the use of context managers to simplify error handling. For instance, it allows the shutter and the connection to the XPS controller to be closed and disconnected automatically in the event of an error occurrence. An example of this case is in the line 24 of the code in Fig. 4, where the shutter is kept open only for the commands in the subsequent indent block, which is actually the line 25. When the code block finishes its execution, either from the normal execution flow or by throwing an exception, a command will be sent automatically for the shutter to be closed. This behavior prevents the shutter from being left open due to the carelessness of the programmer or the lack of appropriate exception handling.

Using an object-oriented approach, the new API reduces code repetition as parameters can be stored as attributes in objects so that they need not to be replicated. An example can be seen in line 16, where the positioner group name ("Group3") appears only once as a parameter. After this definition, the positioner group is directly referenced by the variable "group3." This is advantageous from the programmer's point of view since code verification tools can detect errors that involve variable's names, while typing errors in parameters can remain unnoticed until the code execution.

Other characteristics of the new API include uploading trajectory files automatically to the XPS controller via FTP, checking limits of motion-related parameters for the Newport positioners and consulting the positioner error codes by the module itself.

3.3 Control of Shutter and Laser Power

As shown in Fig. 1, the Thorlabs' SC05 shutter can block or permit the laser beam to be directed to substrates under processing. This on–off shutter operation was previously done manually through the front control panel of the Thorlabs' SC10 shutter controller. In order to incorporate the shutter control into the femtosecond writing system, two automated modes of shutter control were developed one after the other, where the automatic control of shutter could be embedded into either the motion control unit or the automated power adjustment unit. In both situations, the shutter controller should be configured to operate in the external Gate mode, where the control of the shutter will follow the signal on the input trigger BNC connector of the shutter controller. Initially, the idea was only to control simultaneously the positioner movement and the shutter operation during the fabrication process of photonic structures. In this operation mode, the input trigger BNC connector of the shutter controller was connected to a digital output connector of the XPS motion controller. Thus, the shutter control signal is externally provided by the XPS motion controller, which means the shutter control can be embedded into the motion control. Consequently, the shutter will be open when the control signal is active high (TTL) and closed when active low (TTL), which can be specified inside a writing program of photonic structures. Additionally, for that to happen, a simple electronic conditioning circuit was designed to satisfy different voltage requirements of the I/O connectors between the XPS motion controller and the shutter controller. As the shutter

control signal is provided by the XPS, this mode can be named XPS mode. In this way, the XPS controller can control both the shutter and the positioners in a single writing program, which is important to improve production efficiency and reduce time consumption in the case of fabricating repetitive photonic structures, given that there is no need for the human operator to interrupt the writing experiment to close the shutter and reposition the sample for the next writing after finishing the prior one. Similar photonic structures can be written one by one in a single automatic fabrication process. Furthermore, this incorporation of the shutter control into the motion control is necessary for fabricating complex photonic structures that requires immediate shutter control during the positioners' movement.

Formerly, the adjustment of laser power was done by rotating manually the disk attenuator. The transmission ratio of the attenuator varies from 10 to 90%, according to the angular position set by human operators. Every time when the laser power should be configured or changed in the course of a femtosecond writing experiment, the shutter should be closed firstly for the human operator to insert a power sensor into the laser beam path right after the attenuator. Then, the shutter should be opened for the human operator to read the actual value of the laser power with a power meter, which is connected to the power sensor, and set the wanted laser power by rotating the disk attenuator. After that, the shutter should be closed for the human operator to remove the power sensor from the laser beam path. And finally, the shutter should be opened for the experiment to go on. This sequence of operations should be strictly followed in a correct procedure of power adjustment, otherwise it can cause undesired damages to the sample or accidental injuries to human operators, considering that the 800-nm light is invisible to human eyes and the high laser intensity can reach the order of 10^{20} W m^{-2}. Therefore, to automate the power adjustment procedure during a femtosecond fabrication process can avoid such incidents that may result from human misconducts because of carelessness or poor training. Also, an automatic procedure can help reduce human errors and imprecisions that are likely to be introduced into the power measurement with human operations. In addition, with an automated power adjustment sub-system/unit, it can be more time economical and labor saving in circumstances where laser power is the experimental variable for a group of repetitive and time-consuming tests.

Given that the shutter control must be included in a power adjustment procedure, naturally, the shutter control should be embedded into the automated power adjustment unit (PAU). The external TTL input trigger signal for the shutter controller turns to be provided by the PAU instead of the XPS so that this second shutter control mode can be named PAU mode. In fact, the proposal was not to design an automated power adjustment unit separately, but to combine the automated control of shutter and power adjustment with the automated motion control part, which makes possible a totally automated femtosecond writing system, where all experimental parameters can be configured and controlled inside a single writing program. For such a proposal to be accomplished, the PIC microcontroller 16F877A and two stepper motors were applied together with a control program developed in LabVIEW.

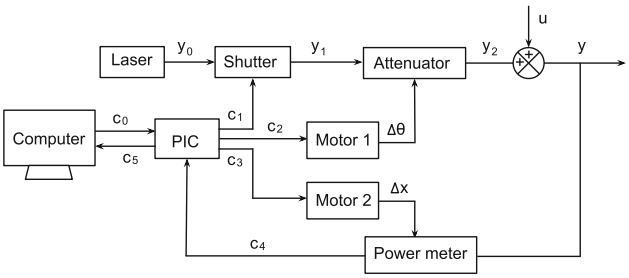

Fig. 5 Functional diagram of the PAU

Figure 5 shows a functional diagram of the automated power adjustment unit. The LabVIEW program runs on a computer, which can receive a power adjustment command and delivers its execution to the PIC microcontroller (c_0). The PIC microcontroller supplies trigger signals (c_1) to the shutter controller and drives the stepper motors (c_2 and c_3). The two stepper motors perform different functions: One is assigned to rotate the disk attenuator ($\Delta\theta$), and the other to place or retrieve the power sensor (Δx). Femtosecond pulses emitted from the laser system (y_0) pass through the shutter (y_1) and the disk attenuator (y_2) that are controlled by the PIC in a closed loop of power adjustment control with the presence of external noise (u). The adjusted power (y) is read by the power meter, and the power value (c_4) is sent to the PIC for processing. The stop criteria for the power adjustment procedure are that the difference between the real value and set point value gets less than 0.4 mW. Then, a power adjustment completion message (c_5) is sent to the writing program to continue undergoing writing experiment. It is worth mentioning that the LabVIEW program and writing program can run independently on different computers or on the same computer and communicate with each other via network socket. Details about the implementation can be found in the reference (Fernandes et al. 2016).

4 Experimental Results and Discussion

4.1 Operational Automated Writing System

As a demonstration of the fully operational automated femtosecond writing system, a writing test is shown in Fig. 6. This test was designed to write four waveguides in a totally

```
1  from xps import XPS
2  from xps.power import PowerCtrl
3  import time
4
5  POSI_ADDRESS  = '192.168.0.254', 5001
6  POWER_ADDRESS = 'localhost', 20551
7  vel_write, vel_return = 0.05, 1
8  power_list = [25, 100, 70, 73]
9  space, length = 0.5, 10
10
11 if __name__ == '__main__':
12     xps = XPS(POSI_ADDRESS)
13     pc = PowerCtrl(POWER_ADDRESS)
14
15     with xps.connected():
16         group3 = xps.group('Group3')
17         group4 = xps.group('Group4')
18         pos3 = group3.positioner()
19         pos4 = group4.positioner()
20
21         for target_power in power_list:
22             pos3.set_sgamma(vel_write, 2500.0,
                   0.02, 0.02)
23             pc.power_ctrl(target_power)
24
25             with pc.shutter_opened():
26                 group3.move_relative(length)
27
28             pos3.set_sgamma(vel_return, 2500.0,
                   0.02, 0.02)
29             group3.move_relative(-length)
30             group4.move_relative(space)
31             time.sleep(1)
```

Fig. 6 Source code for an operational test

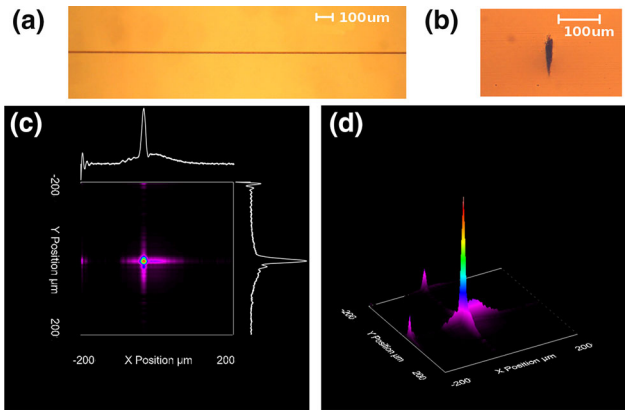

Fig. 7 Microscopy images of an obtained waveguide in **a** top and **b** front views. Near-field guided mode profile of the straight-line waveguide under semiconductor laser injection at 635 nm: **c** 2D intensity map and **d** 3D intensity profile

automatic way, where laser power and sample translation are controlled automatically in a single writing program. In this experiment, the LabVIEW program for the automated power adjustment and the writing program run independently on the same computer and each one is configured with a different communication port, as shown in lines 5–6. Four power values (25, 100, 70 and 73 mW) were required for the writing of four waveguides. All of them follow the same writing procedure that is executed within a repetition loop, as shown in lines 21–31. It starts with configuring motion parameters for a specific positioner that is responsible for the sample translation. Then, the required laser power should be set by sending it as a parameter to a method of the instantiated object of the "PowerCtrl" class. When the LabVIEW program listens to such a request, it commences the automated power adjustment control process. After the target power is reached, a command-completed feedback is returned to the writing program by using the TCP/IP blocking sockets. Thus, the command execution goes on to perform a point-to-point move for a waveguide writing with the use of context manager, which makes sure that the shutter is closed automatically after the movement completion. Then, a higher translation speed is configured to the writing positioner to return to its starting point and sequentially another positioner shifts the sample to the starting point of the next waveguide writing. The expected operational behavior was observed during the experiment, demonstrating that the automated writing system is fully ready for practical use.

4.2 Functional Waveguides

As one of the simplest photonic structures, a waveguide in the form of straight lines can be easily fabricated using a writing program similar to the one shown in Fig. 4. A functional waveguide was written in a quartz sample at a depth of 100 µm below the surface, with a translation speed of 50 µm s^{-1} and a laser power of 15 mW (pulse energy of 15 µJ). The transmission microscope images of the top view and the cross-sectional view of the written waveguide are shown in Fig. 7a, b, with objectives of 4× and 10× magnifications. When635− nm light is injected into the written waveguide, its near-field profiles (XY top-view intensity profile and 3D intensity profile) are shown in Fig. 7c, d. It can be observed from Fig. 7 that the laser-induced modification is uniform along the waveguide axis with an elliptical geometry in the cross section, and the waveguide supports single-mode propagation of 635− nm light, as shown in Fig. 7c, d.

4.3 2D and 3D Photonic Structures

The fabrication of 2D and 3D photonic structures with complex geometries is more complicated due to the bending loss when light is guided in them. Bent regions should be designed carefully with small bend angles or large radius of curvature, which is the crucial and delicate part of designing and engineering for the fabrication of functional photonic structures and devices.

A two-dimensional curved waveguide with two S-bend has been successfully fabricated using the XPS's line–arc trajectories. It was inscribed in a quartz sample at a depth of 100 µm below the surface. The translation speed for the trajectory execution was 5 µm s^{-1}, and the laser power used was 15 mW (pulse energy of 15 µJ). As the schematic shows in Fig. 8a, it contains two S-bend regions and each one consists of two back-to-back arcs. The arc radius (R) and angle (θ) were designed to be 12.013 mm and 2.219°, respectively. Its near-field profiles under laser injection at 635 nm, as shown in Fig. 8b, c, are similar to that of the straight-line waveg-

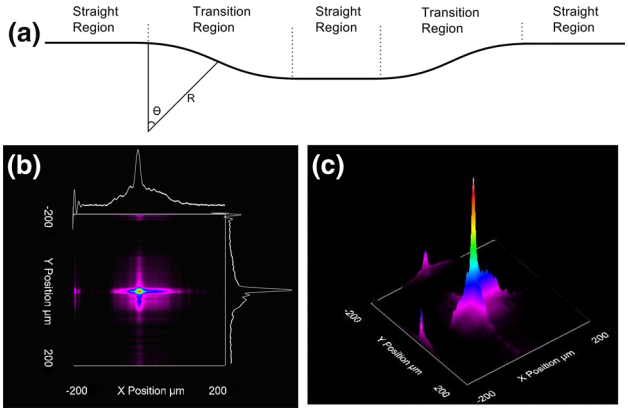

Fig. 8 Schematic representation (**a**) and near-field guided mode profiles (**b**, **c**) of a S-bend waveguide

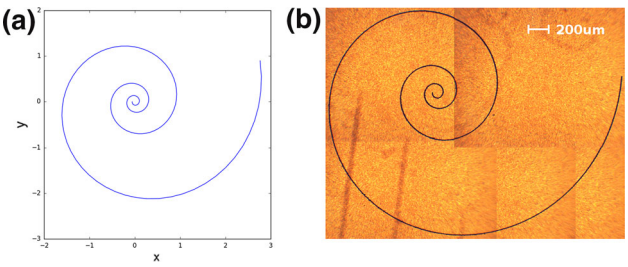

Fig. 9 Graphical representation (**a**) and transmission microscope image (**b**) of a logarithmic spiral trajectory

uide, demonstrating its ability of guiding light. Furthermore, it is proposed for a future fabrication of directional couplers, which are actually made up of two S-bend waveguides of this kind with symmetry.

In order to demonstrate that the automated writing system is capable of inscribing structures of complex and arbitrary geometries, a logarithmic spiral pattern (2D) is written at the surface of a microscope slide, using the XPS's spline trajectory. It is worth mentioning that it was proposed to show that the spline trajectory really allows tracing a smooth path of arbitrary form instead of aiming to produce a light-guiding structure. As the parametric form of this self-similar spiral curve is well known, a trajectory file can be generated with a simple mathematical program, which contains predefined trajectory points that should be hit when the trajectory is executed by the motion controller. With the generated trajectory file, a graphical representation of the spiral trajectory can be plotted, which is shown in Fig. 9a. The transmission microscope image of the traced spiral path is shown in Fig. 9b, with an objective of 4× magnification. It can be found that the graphical geometry is very similar to the spiral path that is obtained in reality with the irradiation of femtosecond pulses.

Moreover, as a demonstration of the spline trajectory's ability to trace smooth 3D curves of arbitrary geometries, a fan-out device reported in the reference (Thomson et al. 2008) has been written into a microscope slide, where four waveguides were inscribed sequentially in a single-sweep process. It was originally designed to allow each core of a 2 × 2 multicore fiber (MCF) to be addressed individually by one of four single-mode fibers held in a 4 × 1 fiber V-groove array (FVA). Figure 10 shows a graphical representation of the fan-out structure, which is plotted from a developed mathematical program using its original structural parameters referred in the literature. Each of the four waveguides is made up of three linear sections. The run-in section and the run-out section have the same length of 2.5 mm, while the middle section has a length of 20 mm along the *Y* axis. At the MCF coupling end, the four run-in sections were arranged in a 50 µm × 50 µm array, whereas the four run-out sections were arranged in a one-dimensional array with a 250-µm spacing at the FVA coupling end of the fan-out. However, it should be noticed that the graphical representation in Fig. 10 is not proportional to the real dimension, as it is made intendedly in order to provide a better visualization of the structural form.

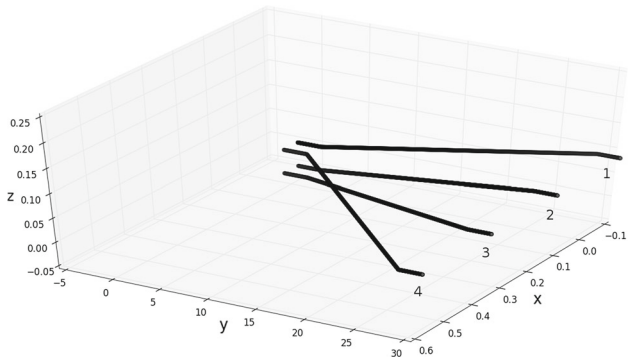

Fig. 10 Graphical representation of a 3D fan-out structure

With the aid of a confocal microscope, sets of images can be obtained at different depths for the reconstruction of three-dimensional structures. Four sets of representative microscope images of the fan-out structure were taken with an objective of 4× magnification, which are shown in Fig. 11, where a top view is shown on the left and a side view on the right. Figure 11a, d refers to the run-in and run-out sections of the fan-out structure, while Fig. 11b, c refers to the entering part and the exiting part of the middle section, respectively. In the run-in section, waveguides 1 and 4 lie exactly below waveguides 2 and 3 so that in a top view only two waveguides (2 and 3) are visible, as shown in Fig. 11a. Due to the elongated shape of the cross section of waveguides, as shown in Fig. 7b, the upper waveguides (2 and 3) can not be distinguished from the lower ones (1 and 4) in the side view in the Fig. 11a. In the middle section, each waveguide follows a distinct path in a way that the fan-out structure branches out along the *X*-axis. As to their related microscope images, waveguides trend to separate from each other more and more along the *Y*-axis, as shown in Fig. 11b, c. Also, it

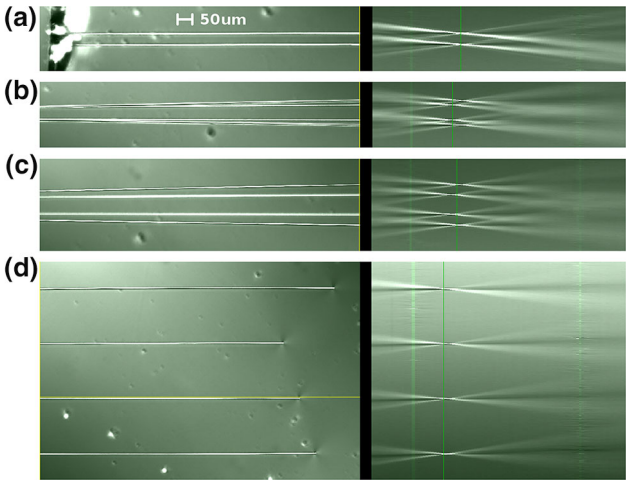

Fig. 11 Confocal microscope images of a fan-out structure produced with the automated femtosecond written system. The green lines in the right images indicate locations of the sample's top surface, the focus of objective and the sample's bottom surface. For details of each image, refer to the text (Color figure online)

can be observed that the upper waveguides (2 and 3) locate on the same level, and the same to the lower waveguides (1 and 4). However, the former depth differs from the latter. In the run-out section, the four waveguides run parallel with each other at the same depth, as shown in Fig. 11d.

5 Conclusion

In conclusion, this work proposes an automated writing system, which is developed for the fabrication of photonic structures with femtosecond pulses. It enables the fabrication process to be totally computer controlled, turning the fabrication process more precise, secure, time economical and labor saving. More importantly, it makes possible the fabrication of photonic structures with complex and arbitrary geometries in the field of integrated optics and three-dimensional optical circuits. The development aspect has been described to exhibit how each control unit works as well as how the motion-related and laser-related controls can be integrated into a single writing program that controls automatically fabrication processes. Using the developed automated system, functional straight-line and S-bend waveguides have been successfully fabricated. The possibility of writing 2D and 3D complex photonic structures is also confirmed with the demonstration of writing a logarithmic spiral path (2D) and a fan-out structure (3D). However, in order to obtain 2D and 3D functional photonic devices, future effort will be dedicated to the experimental part, where experimental parameters and structural design for a desired photonic device should be tested, verified and modified repeatedly until the expected function is reached.

Acknowledgements The authors acknowledge support and assistance received from the Federal University of Technology - Paraná(UTFPR) and Brazilian government agencies of Coordenação de Aperfeiçoamento de Pessoal de Nível Superior (CAPES), Conselho Nacional de Desenvolvimento Científicoe Tecnológico (CNPq, process 4004414/2013-9, 470430/2013-3 and 448728/2014-1), Financiadora de Estudos e Projetos (FINEP) and Fundação Araucária. Thanks also go to Lucas Lugnani Fernandes and Henrique Napolião Barreto for their co-work and contribution in implementing the automated power adjustment unit for the final integration of the automated femtosecond writing system.

References

Ams, M., Marshall, G., Spence, D., & Withford, M. (2005). Slit beam shaping method for femtosecond laser direct-write fabrication of symmetric waveguides in bulk glasses. *Optics Express*, *13*(15), 5676–5681. https://doi.org/10.1364/OPEX.13.005676.

Chen, W. J., Eaton, S. M., Zhang, H., & Herman, P. R. (2008). Broadband directional couplers fabricated in bulk glass with high repetition rate femtosecond laser pulses. *Optics Express*, *16*(15), 11470. https://doi.org/10.1364/OE.16.011470.

Davis, K. M., Miura, K., Sugimoto, N., & Hirao, K. (1996). Writing waveguides in glass with a femtosecond laser. *Optics Letters*, *21*(21), 1729–1731.

Eaton, S. M., Ng, M. L., Osellame, R., & Herman, P. R. (2011). High refractive index contrast in fused silica waveguides by tightly focused, high-repetition rate femtosecond laser. *Journal of Non-Crystalline Solids*, *357*(11–13), 2387–2391. https://doi.org/10.1016/j.jnoncrysol.2010.11.082.

Fernandes, L. L., Barreto, H. N., Bertogna, E. G., Assef, A. A., & Chiamenti, I. (2016) A laser beam power adjustment system control and automation. In *2016 12th IEEE international conference on industry applications (INDUSCON)* (pp. 1–8). https://doi.org/10.1109/INDUSCON.2016.7874599

Gattass, R. R., & Mazur, E. (2008). Femtosecond laser micromachining in transparent materials. *Nature Photonics*, *2*(4), 219–225. https://doi.org/10.1038/nphoton.2008.47.

Lacraz, A., Polis, M., Theodosiou, A., Koutsides, C., & Kalli, K. (2015). Bragg grating inscription in cytop polymer optical fibre using a femtosecond laser (Vol. 9507, pp. 95070K–95070K–6)

Liu, J., Zhang, Z., Chang, S., Flueraru, C., & Grover, C. P. (2005). Directly writing of 1-to-n optical waveguide power splitters in fused silica glass using a femtosecond laser. *Optics Communications*, *253*(4), 315–319.

Marshall, G. D., Ams, M., & Withford, M. J. (2006). Direct laser written waveguide-Bragg gratings in bulk fused silica. *Optics Letters*, *31*(18), 2690–2691. https://doi.org/10.1364/OL.31.002690.

Mauclair, C., Cheng, G., Huot, N., Audouard, E., Rosenfeld, A., Hertel, I. V., et al. (2009). Dynamic ultrafast laser spatial tailoring for parallel micromachining of photonic devices in transparent materials. *Optics Express*, *17*(5), 3531. https://doi.org/10.1364/OE.17.003531.

Minoshima, K., Kowalevicz, A., Ippen, E., & Fujimoto, J. (2002). Fabrication of coupled mode photonic devices in glass by nonlinear femtosecond laser materials processing. *Optics Express*, *10*(15), 645. https://doi.org/10.1364/OE.10.000645.

Miura, K., Qiu, J., Inouye, H., Mitsuyu, T., & Hirao, K. (1997). Photowritten optical waveguides in various glasses with ultrashort pulse laser. *Applied Physics Letters*, *71*(23), 3329–3331.

Nolte, S., Will, M., Burghoff, J., & Tuennermann, A. (2003). Femtosecond waveguide writing: A new avenue to three-dimensional integrated optics. *Applied Physics A: Materials Science & Processing*, *77*(1), 109–111. https://doi.org/10.1007/s00339-003-2088-6.

Pospiech, M., Emons, M., Steinmann, A., Palmer, G., Osellame, R., Bellini, N., et al. (2009). Double waveguide couplers produced by simultaneous femtosecond writing. *Optics Express*, *17*(5), 3555–3563. https://doi.org/10.1364/OE.17.003555.

Sakakura, M., Sawano, T., Shimotsuma, Y., Miura, K., & Hirao, K. (2010). Fabrication of three-dimensional 1×4 splitter waveguides inside a glass substrate with spatially phase modulated laser beam. *Optics Express*, *18*(12), 12136–12143.

Sikorski, Y., Said, A. A., Bado, P., Maynard, R., Florea, C., & Winick, K. A. (2000). Optical waveguide amplifier in nd-doped glass written with near-ir femtosecond laser pulses. *Electronics Letters*, *36*(3), 226–227. https://doi.org/10.1049/el:20000172.

Thomson, R. R., Bookey, H. T., Psaila, N. D., Fender, A., Campbell, S., Macpherson, W. N., et al. (2008). Ultrafast laser inscription of a three dimensional fan-out device for multicore fiber coupling applications. In *2008 conference on lasers and electro-optics and 2008 conference on quantum electronics and laser science* (pp. 1–2). https://doi.org/10.1109/CLEO.2008.4552346

Valle, G. D., Osellame, R., Chiodo, N., Taccheo, S., Cerullo, G., Laporta, P., et al. (2005). C-band waveguide amplifier produced by femtosecond laser writing. *Optics Express*, *13*(16), 5976–5982. https://doi.org/10.1364/OPEX.13.005976.

Zhou, K., Dubov, M., Mou, C., Zhang, L., Mezentsev, V. K., & Bennion, I. (2010). Line-by-line fibra bragg grating made by femtosecond laser. *IEEE Photonics Technology Letters*, *22*(16), 1190–1192.